

## Error-Speed Correlations in Biopolymer Synthesis

Davide Chiuchiu,<sup>1</sup> Yuhai Tu,<sup>2</sup> and Simone Pigolotti<sup>1,\*</sup>

<sup>1</sup>*Biological Complexity Unit, Okinawa Institute of Science and Technology Graduate University, Onna, Okinawa 904-0495, Japan*

<sup>2</sup>*IBM T.J. Watson Research Center, Yorktown Heights, New York 10598, USA*



(Received 6 February 2019; published 19 July 2019)

Synthesis of biopolymers such as DNA, RNA, and proteins are biophysical processes aided by enzymes. The performance of these enzymes is usually characterized in terms of their average error rate and speed. However, because of thermal fluctuations in these single-molecule processes, both error and speed are inherently stochastic quantities. In this Letter, we study fluctuations of error and speed in biopolymer synthesis and show that they are in general correlated. This means that, under equal conditions, polymers that are synthesized faster due to a fluctuation tend to have either better or worse errors than the average. The error-correction mechanism implemented by the enzyme determines which of the two cases holds. For example, discrimination in the forward reaction rates tends to grant smaller errors to polymers with faster synthesis. The opposite occurs for discrimination in monomer rejection rates. Our results provide an experimentally feasible way to identify error-correction mechanisms by measuring the error-speed correlations.

DOI: [10.1103/PhysRevLett.123.038101](https://doi.org/10.1103/PhysRevLett.123.038101)

Organisms encode genetic information in heteropolymers such as DNA and RNA. Replication of these heteropolymers is a nonequilibrium process catalyzed by enzymes. The crucial observables to characterize these enzymes are their error rate and speed. A low error rate, defined as the fraction of monomers in the copy that do not match the template, ensures the correct transmission of biological information. High processing speed is also crucial to guarantee fast cell growth. Theoretical approaches have been developed to compute the average error and average speed of the polymerization processes [1–7]. However, at the single molecule level, both error and speed can present significant stochastic fluctuations.

In this Letter we address fluctuations in the error and speed of polymer synthesis. In particular, we show that correlations between these quantities exist. These correlations provide a way to identify the error correction mechanism adopted by an enzyme from experimental data. This approach can circumvent the characterization of these enzymes by measuring all kinetic rates of the underlying reaction network [8–15].

We consider an enzyme that replicates an existing template polymer by sequentially incorporating monomers into a copy polymer [Fig. 1(a)]. In a given time interval  $T$ , the enzyme synthesizes a copy made up of a number of monomers  $L$ . Because of thermal fluctuations, enzymes sometimes incorporate wrong monomers ( $w$ ) that do not match the template, instead of the right ones ( $r$ ). In practical cases, there can be multiple types of wrong monomers; for simplicity, we do not distinguish among them. We denote  $R$  as the number of right matches and  $W$  the number of wrong matches in the copy, so that  $R + W = L$ . The error of the polymer copy can be then expressed as

$$\eta = \frac{W}{L}. \quad (1)$$

We focus on two possible setups, corresponding to two idealized experiments. In the first, the enzyme replicates a given template polymer for a fixed time  $T \gg 1$ . [Fig. 1(b)]. Because of the stochasticity of single-molecule biochemical reactions, both the polymer length  $L$  and the error  $\eta$  fluctuate. We denote their variance with  $\sigma_L^2 = \langle L^2 \rangle - \langle L \rangle^2$ ,  $\sigma_\eta^2 = \langle \eta^2 \rangle - \langle \eta \rangle^2$ , and their covariance with  $\sigma_{\eta L}^2 = \langle \eta L \rangle - \langle \eta \rangle \langle L \rangle$ , where  $\langle \dots \rangle$  is an average over different realizations of the same process. Since  $T$  is fixed, we quantify the correlations between error and speed with the error-length coefficient

$$r_{\eta L} = \frac{\sigma_{\eta L}^2}{\sigma_L \sigma_\eta}. \quad (2)$$

In the second setup, each realization terminates when the enzyme has incorporated a number  $L \gg 1$  of monomers [Fig. 1(c)]. In this case,  $L$  is fixed, whereas the total duration  $T$  of the copy process fluctuates. This setup represents the biological scenario where an enzyme copies a polymer of fixed length. In this case, we study the correlation between the polymerization error and speed via the coefficient

$$r_{\eta T} = \frac{\sigma_{\eta T}^2}{\sigma_T \sigma_\eta}, \quad (3)$$

where  $\sigma_T^2 = \langle T^2 \rangle - \langle T \rangle^2$  is the variance of  $T$  and  $\sigma_{\eta T}^2 = \langle \eta T \rangle - \langle \eta \rangle \langle T \rangle$ .

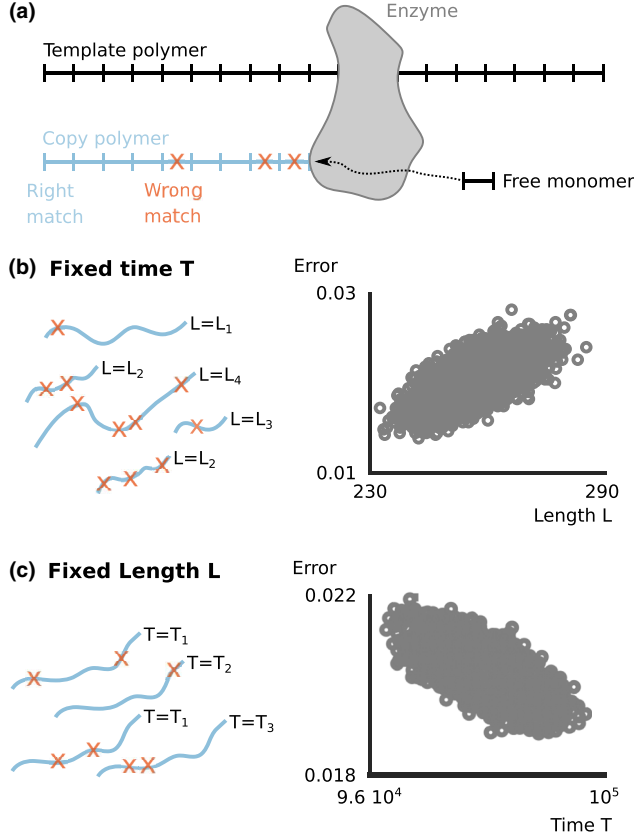


FIG. 1. (a) An enzyme reads an existing heteropolymer as a template and sequentially incorporates monomers to copy it. Each incorporated monomer can either be a right ( $r$ ) or wrong ( $w$ ) match with the template polymer. (b) Because of thermal fluctuations, the polymer length  $L$  and error  $\eta$  are random quantities at fixed completion time  $T$ . (c) When an enzyme produces a copy polymer with fixed length, the error  $\eta$  and the time  $T$  fluctuate. Scatterplots in (b) and (c) represent  $N = 5000$  realizations of the same polymerization process where incorporation occurs via two sequential irreversible reactions; see Supplemental Material [16]. Data skewness indicates correlations in the observables.

Our two setups are akin to two conjugate ensembles in equilibrium statistical physics. For large times (and lengths), fluctuations in these two ensembles can be related by means of large deviation theory [21]. Following this approach we obtain

$$r_{\eta T} = -r_{\eta L} \quad (4)$$

(see Supplemental Material [16] for details). Equation (4) implies that the two setups correspond to two equivalent ensembles. Therefore, in the following we will focus on the fixed time setup only.

To estimate  $r_{\eta L}$  we first observe that the distributions of  $R$  and  $W$  tend to Gaussian for large  $T$  due to the central limit theorem. We can therefore obtain the moments of  $L = R + W$  and  $\eta = W/(W + R)$  from those of  $R$  and  $W$ . This procedure yields

$$r_{\eta L} = \frac{(1 - 2\langle\eta\rangle)\sigma_{RW}^2 + (1 - \langle\eta\rangle)\sigma_W^2 - \langle\eta\rangle\sigma_R^2}{\sqrt{\sigma_R^2\sigma_W^2 - (\sigma_{RW}^2)^2}}, \quad (5)$$

where  $\sigma_R^2$ ,  $\sigma_W^2$ , and  $\sigma_{RW}^2$  are the variances and covariance of  $R$  and  $W$ . To compute the quantities in Eq. (5), we assume that the final chemical reaction to incorporate a  $r$  or a  $w$  monomer is irreversible. This assumption is realistic for most practical cases such as DNA polymerization [14,22] and protein translation [8–10]. Our framework could be generalized to cases where the last reaction is reversible, permitting an interpretation of the results using stochastic thermodynamics [1–5,23]. For simplicity, we also assume that probabilities to incorporate right and wrong matches do not depend on the template monomer. Under these assumptions, we describe the polymerization process by means of the probabilities  $\eta_0$  and  $1 - \eta_0$  to incorporate a wrong ( $w$ ) or a right ( $r$ ) monomer, respectively, and the probability distributions  $P(\tau|r)$  and  $P(\tau|w)$  that it takes a time  $\tau$  to incorporate an  $r$  or a  $w$  monomer, respectively. The value of  $\eta_0$  and the functions  $P(\tau|r)$  and  $P(\tau|w)$  can be computed from the underlying reaction network [6,24]. With these quantities we can express the joint probability  $P(R, W|T)$  for large fixed  $T$  as

$$P(R, W|T) \approx \binom{R+W}{W} \eta_0^W (1 - \eta_0)^R \times \int_0^\infty \prod_{i=1}^R \prod_{j=1}^W d\tau_i d\tau_j P(\tau_i|r) P(\tau_j|w) \times \delta\left(\sum_{n=1}^R \tau_n + \sum_{m=1}^W \tau_m - T\right). \quad (6)$$

In Eq. (6), the binomial term weights the probability of incorporating  $R$  right and  $W$  wrong monomers. The integral term in the second line selects trajectories whose sum of incorporation times is equal to  $T$ .

Evaluating the average error for large  $T$  gives the consistency relation  $\langle\eta\rangle = \eta_0$ . Computing the covariance matrix of  $P(R, W|T)$  in the same limit, see Supplemental Material [16], and substituting the resulting moments in Eq. (5) gives

$$r_{\eta L} = \frac{\beta}{\sqrt{1 + \beta^2}}, \quad (7)$$

with

$$\beta = \frac{(\langle\tau\rangle_r - \langle\tau\rangle_w)\sqrt{\eta_0(1 - \eta_0)}}{\sqrt{(1 - \eta_0)\sigma_{\tau,r}^2 + \eta_0\sigma_{\tau,w}^2}}, \quad (8)$$

where  $\langle\tau\rangle_r$ ,  $\langle\tau\rangle_w$ ,  $\sigma_{\tau,r}^2$ , and  $\sigma_{\tau,w}^2$  are the means and variances of  $P(\tau|r)$  and  $P(\tau|w)$ , that we assume to be finite. We validated Eqs. (7) and (8) with stochastic simulations (see Supplemental Material [16]) and we will use them to

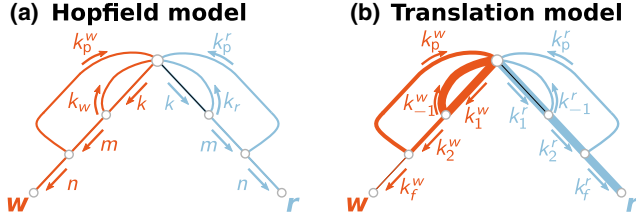


FIG. 2. Reaction networks for polymer synthesis. (a) Hopfield model. The kinetic rates satisfy the relations  $k_r = k \exp[\Delta E_r/k_B T]$ ,  $k_w = k \exp[\Delta E_w/k_B T]$ ,  $k_p^r = m \exp[\Delta E_r/k_B T]$  and  $k_p^w = m \exp[\Delta E_w/k_B T]$  with  $k \gg 1$ ,  $m = 1$ , and  $n \ll 1$ , so that the model operates in the proofreading regime [25]. (b) Protein translation model from Ref. [24] with rates extracted from Ref. [10]. Same line thickness marks reaction rates of the same order of magnitude.

compute error-speed correlations in the following. Expanding Eq. (8) and Eq. (7) for small  $\eta_0$  leads to

$$r_{\eta L} \approx \frac{\langle \tau \rangle_r - \langle \tau \rangle_w}{\sigma_{\tau, r}} \sqrt{\eta_0}. \quad (9)$$

Equation (9) is our main result. It predicts that the sign of  $r_{\eta L}$  depends on the sign of  $(\langle \tau \rangle_r - \langle \tau \rangle_w)$  only. We will show that, in practice, the error correction mechanisms determine this sign.

**Kinetic proofreading.**—Hopfield’s kinetic proofreading model [25] is an elegant example of incorporation processes implementing error correction. In this model, the enzyme first captures either an  $r$  or  $w$  monomer [Fig. 2(a)]. After the initial binding, the enzyme can either reject the monomer or consume ATP to induce a conformational change. Thanks to this change, the enzyme gains a second chance to reject wrong monomers. This second rejection reaction is the kinetic proofreading and it greatly reduces the error probability  $\eta_0$ . This idea has been generalized to more complex proofreading models [2,6,24,26–29]. Rates of forward reactions in the Hopfield model do not depend on the monomer type, whereas rejection reactions have higher rates for  $w$  than  $r$  monomers [Fig. 2(a)]. In the proofreading regime [Fig. 2(a)], the error probability  $\eta_0$  can be estimated with first passage time techniques [24] as

$$\eta_0 \approx \left(1 + \frac{k_r k_p^r}{k_w k_p^w}\right)^{-1} \approx e^{-[2(\Delta E_w - \Delta E_r)/k_B T]}, \quad (10)$$

where the ratios  $k_r/k_w$  and  $k_p^r/k_p^w$  reflect the discrimination in the rejection rates (see Refs. [25] and Supplemental Material [16]),  $k_B$  is the Boltzmann constant, and  $T$  is the temperature. Both these ratios relate to the difference  $\Delta E_r - \Delta E_w$  in binding energy of  $r$  and  $w$  monomers through  $k_r/k_w = k_p^r/k_p^w = \exp[(\Delta E_r - \Delta E_w)/k_B T]$ . Outside of the error correction regime, the error is always larger than predicted by Eq. (10) [25,30]. In the proofreading regime of the Hopfield model, error and speed

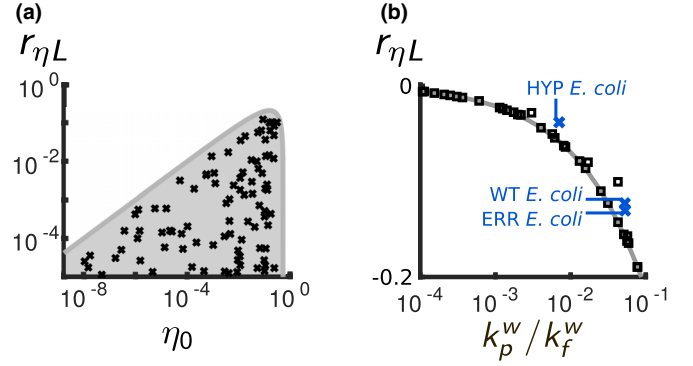


FIG. 3. The Hopfield model and the protein translation model have opposite error-speed correlations. (a) Hopfield model. The gray shaded region defines the allowed values of  $r_{\eta L}$  for a given error probability  $\eta_0$ , see Eq. (11). Black crosses are estimates of  $\eta_0$  and  $r_{\eta L}$  for 60 random sets of reaction rates in the proofreading regime (see caption of Fig. 2, Supplemental Material [16], and Table S2). (b) Protein translation. To test whether Eq. (13) (gray line) is a good approximation of simulated values of the error-speed coefficient, we computed  $r_{\eta L}$  corresponding to the kinetic rates in Ref. [24] for wild type *E. coli*, a hypercorrective and an error-prone mutation (blue crosses). We also evaluated  $r_{\eta L}$  for randomly generated sets of the reaction rates in Fig. 2(b) (black squares). For all points in both panels, correlation coefficients are evaluated by means of Eqs. (7)–(8) upon computing moments of incorporation times with first passage time techniques [24]. See the Supplemental Material [16] for details of numerical calculations.

fluctuations are positively correlated. In particular, the error-length coefficient always falls in the range

$$0 \leq r_{\eta L} \leq \eta_0 \left( \sqrt{\frac{1 - \eta_0}{\eta_0}} - 1 \right) \quad (11)$$

for any choice of  $\eta_0$ , see Supplemental Material [16] and Fig. 3. This implies that the error-speed correlations become negligible when proofreading ensures very small errors.

**Protein translation.**—A standard model of protein translation is characterized by the same reactions of the Hopfield model [Fig. 2(b) and Refs. [24,31,32]]. A major difference is that forward reactions discriminate between the  $r$  and  $w$  monomers (Table S1 [16] and Refs. [10,24]). Within this model we estimate the error probability as

$$\eta_0 \approx \frac{k_f^w}{k_f^r} \left( 1 + \frac{k_f^w}{k_p^w} \right)^{-1} \quad (12)$$

(see Refs. [24] and Supplemental Material [16]). In this case, the error probability depends on the relative preference to bind  $r$  rather than  $w$  monomers (term  $k_f^w/k_f^r$ ). Proofreading effectiveness over the incorporation reaction for  $w$  monomers (term  $k_f^w/k_p^w$ ) further decreases the error

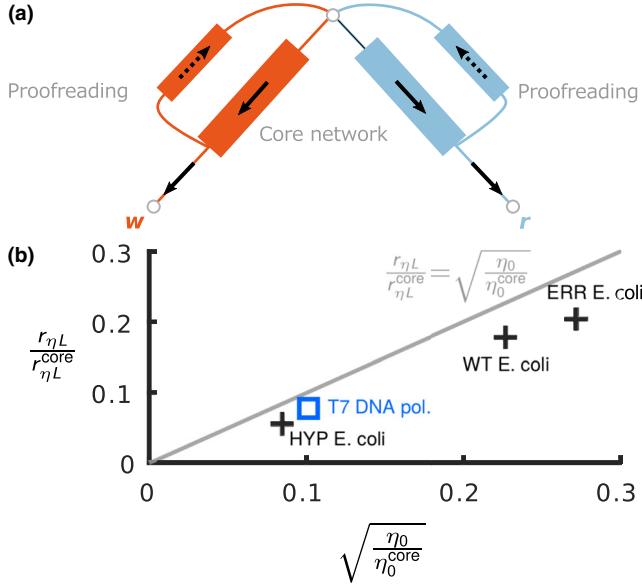


FIG. 4. Proofreading suppresses the error-speed correlations. (a) Incorporation with a core network complemented by proofreading reactions. Each block in the figure represents an arbitrary subnetwork with an average flux in the direction of the arrows. (b) Comparison of Eq. (14) (solid line) with computation of error-speed correlations from measured kinetic rates, see Ref. [16]. We considered the ribosomes in three strains of *E. coli*: wild type, hypercorrective, and error prone [10,24]. For each strain, we built the core network by removing the proofreading reactions and computed the relative change in  $r_{\eta L}$  and  $\eta_0$  between the original and core networks. We performed the same analysis for a model of T7 DNA polymerase (blue square, see Ref. [16] and [12]). The data qualitatively agree with Eq. (14).

probability. Because of the discrimination in the forward rates, the energy difference  $\Delta E_r - \Delta E_w$  does not set a lower bound to the error probability as in the Hopfield model [6]. Similar calculations as in Eq. (11) predict an error-length coefficient

$$r_{\eta L} \approx -\frac{1}{\sqrt{2}} \left( 1 + \frac{k_p^w}{k_f^w} \right)^{-1/2}. \quad (13)$$

(Supplemental Material [16] and Fig. 3). At variance with the Hopfield model, the error-length coefficient is always negative in protein translation. This striking difference arises from the discrimination in the forward rates, as further clarified in the following. Also in this case, the absolute value of the error-speed correlations decreases at increasing proofreading efficiency. Ribosomes with impaired kinetic proofreading should then exhibit stronger error-speed correlations. A computation of error-speed correlations from experimentally measured rates for different *E. coli* strains supports Eq. (13), Fig. 3.

**Core network.**—In both models we considered, kinetic proofreading reduces the absolute value of the error-length coefficient without changing its sign. To show this effect in

general, we consider an arbitrary reaction network where we identify some of the reaction steps as those implementing kinetic proofreading [Fig. 4(a)]. For example, in both models of Fig. 2, the proofreading reactions are those with rates  $k_p^r$  and  $k_p^w$ . The complete network has an error probability  $\eta_0$  and an error-length coefficient  $r_{\eta L}$ . We now remove all the proofreading reactions and define the remaining reactions as the “core network.” In many practical cases the core network is a simple linear chain of reactions, so that it is easy to compute its error probability  $\eta_0^{\text{core}}$  and its error-length coefficient  $r_{\eta L}^{\text{core}}$ . To compare  $r_{\eta L}$  and  $r_{\eta L}^{\text{core}}$  we assume that both  $\eta_0$  and  $\eta_0^{\text{core}}$  are small so that Eq. (9) holds. We further assume that proofreading is a relatively rare event that does not significantly influence the incorporation times. Taking the ratio  $r_{\eta L}/r_{\eta L}^{\text{core}}$  we therefore obtain

$$r_{\eta L} \approx \sqrt{\frac{\eta_0}{\eta_0^{\text{core}}}} r_{\eta L}^{\text{core}}. \quad (14)$$

Since proofreading reduces the error probability ( $\eta_0 < \eta_0^{\text{core}}$ ), it also reduces the absolute value of the error-length coefficient without changing its sign. We tested our prediction by computing  $r_{\eta L}$  from experimentally measured kinetic rates in *E. coli* ribosomes (Table S1 in the Supplemental Material [16], and Refs. [10,24]) and from the T7 DNA polymerase [14] (see Fig. S1 in the Supplemental Material [16] for the T7 datum). Equation (14) qualitatively captures the dependence of the error-length coefficient on the error-correction effectiveness [Fig. 4(b)]. Quantitative discrepancies arise because the assumption that proofreading does not affect incorporation times partially breaks down.

The core-network approach qualitatively explains why the error-speed correlations have different signs in the Hopfield model [Fig. 2(a)] and in the protein translation model [Fig. 2(b)]. Because of the discrimination in the backward rates,  $r$  monomers bind to the enzyme for a long time in the core network of the Hopfield before the final incorporation. On the other hand,  $w$  monomers bind to the enzyme for a short time before they are either rejected or incorporated. This implies that  $r_{\eta L}^{\text{core}} > 0$  and therefore  $r_{\eta L} > 0$ , as showed in Fig. 3. Conversely, the discrimination in the forward rates grants a fast incorporation of  $r$  monomers in the core network of the protein translation model. Thus,  $r_{\eta L}^{\text{core}} < 0$  and  $r_{\eta L} < 0$ , consistently with Eq. (13).

In this Letter we studied the correlations of the empirical error in a copy polymer and its synthesis speed. These correlations probe general features of error-correction and permit us to classify error-correction mechanisms into two broad categories: those leading to positive or to negative error-speed correlations. We showed that the Hopfield model [25] and a model of protein translation with discrimination in the forward rates [8–10,31,33] belong



to opposite categories. Furthermore, a model of T7 DNA polymerase with forward discrimination [14] belongs to the same category of the protein translation model (see Supplemental Material [16]). This suggests that measurements of the error-speed correlations could reveal the presence of forward discrimination in replicative enzymes. Cell-free translation systems [34,35] could provide simple and versatile *in vitro* assays to perform these measurements for ribosomes. A possible experiment would be to let the system translate a given protein for a fixed short time, separate the products into shorter and longer peptides, and then quantify errors by measuring the peptide composition in each class, for example, using mass spectroscopy. Similar experiments for DNA polymerases could bring insight into poorly characterized chemical reaction networks, such as those of human mitochondrial DNA pol- $\gamma$  [36], yeast pol- $\epsilon$  [37], and pol- $\delta$  [38,39].

The magnitude of the error-speed correlations decreases when proofreading effectiveness increases. This implies that proofreading-deficient enzymes [36–39] and *in vitro* assays that favor misincorporation [15,33] are best suited to test our theory, for two reasons. First, the increased magnitude of error-speed correlations in the absence of error correction makes them easier to measure. Second, the poor precision of proofreading-deficient enzymes [14] reduces the sample size needed to empirically estimate error fluctuations.

Our result may also have consequences for the evolution of genomes. Recent work showed that the cells which replicates earlier thanks to environmental fluctuations, contribute more to population growth [40]. With significant error-speed correlations, the growth of a population could then be driven by the individuals whose DNA and proteins have significantly different error fractions from the population average. This phenomenon could have played a role in early stages of life.

We underline the conceptual difference between our results and the speed-error trade-off [5,6,24,30], in particular as observed in protein translation [31,33,41]. In translation, tuning the concentration of  $Mg^{++}$  ions provokes an approximately linear trade-off between the average error and the average reaction speed [31]. These kinds of trade-offs may depend on the choice of a control parameter [6,24]. In contrast, we have shown that fluctuations of velocity and error are negatively correlated in protein translation for fixed external parameters. It remains to be explored whether the two results can be generally connected in a similar fashion as equilibrium fluctuations and responses to external forces are related in statistical physics [42,43].

We thank Michael Baym, Lucas Carey, Antonio Celani, Massimo Cencini, Todd Gingrich, and Jordan Horowitz for discussion. We further thank S. Aird and P. Laurino for comments on the manuscript. This work was supported by JSPS KAKENHI Grant No. JP18K03473 (to D.C. and S.P.), and by NIH Grant No. R01-GM081747 (to Y.T.).

\*simone.pigolotti@oist.jp

- [1] C. H. Bennett, *BioSystems* **11**, 85 (1979).
- [2] D. Andrieux and P. Gaspard, *Proc. Natl. Acad. Sci. U.S.A.* **105**, 9516 (2008).
- [3] F. Cady and H. Qian, *Phys. Biol.* **6**, 036011 (2009).
- [4] M. Esposito, K. Lindenberg, and C. Van den Broeck, *J. Stat. Mech.: Theory Exp.* (2010) P01008.
- [5] P. Sartori and S. Pigolotti, *Phys. Rev. X* **5**, 041039 (2015).
- [6] S. Pigolotti and P. Sartori, *J. Stat. Phys.* **162**, 1167 (2016).
- [7] P. Gaspard, *Phys. Rev. Lett.* **117**, 238101 (2016).
- [8] K. B. Gromadski and M. V. Rodnina, *Mol. Cell* **13**, 191 (2004).
- [9] H. S. Zaher and R. Green, *Cell* **136**, 746 (2009).
- [10] T. Pape, W. Wintermeyer, and M. Rodnina, *EMBO J.* **18**, 3800 (1999).
- [11] H. L. Gahlon, A. R. Walker, G. A. Cisneros, M. H. Lamers, and D. S. Rueda, *Phys. Chem. Chem. Phys.* **20**, 26892 (2018).
- [12] T. A. Kunkel and K. Bebenek, *Annu. Rev. Biochem.* **69**, 497 (2000).
- [13] T. A. Kunkel and D. A. Erie, *Annu. Rev. Genet.* **49**, 291 (2015).
- [14] M. F. Goodman, S. Creighton, L. B. Bloom, J. Petruska, and D. T. A. Kunkel, *Crit. Rev. Biochem. Mol. Biol.* **28**, 83 (1993).
- [15] M. V. Rodnina and W. Wintermeyer, *Annu. Rev. Biochem.* **70**, 415 (2001).
- [16] See Supplemental Material at <http://link.aps.org/supplemental/10.1103/PhysRevLett.123.038101>, which includes Refs. [17–20], for additional details and mathematical calculations.
- [17] C. Gardiner, *Stochastic Methods: A Handbook for the Natural and Social Sciences*, Springer Series in Synergetics (Springer, Berlin, Heidelberg, 2009).
- [18] H. Touchette, *Phys. Rep.* **478**, 1 (2009).
- [19] S. Redner, *A Guide to First-Passage Processes*, A Guide to First-passage Processes (Cambridge University Press, Cambridge, England, 2001).
- [20] D. T. Gillespie, *J. Comput. Phys.* **22**, 403 (1976).
- [21] T. R. Gingrich and J. M. Horowitz, *Phys. Rev. Lett.* **119**, 170601 (2017).
- [22] S. S. Patel, I. Wong, and K. A. Johnson, *Biochemistry* **30**, 511 (1991).
- [23] J. M. Poulton, P. R. ten Wolde, and T. E. Ouldridge, *Proc. Natl. Acad. Sci. U.S.A.* **116**, 1946 (2019).
- [24] K. Banerjee, A. B. Kolomeisky, and O. A. Igoshin, *Proc. Natl. Acad. Sci. U.S.A.* **114**, 5183 (2017).
- [25] J. J. Hopfield, *Proc. Natl. Acad. Sci. U.S.A.* **71**, 4135 (1974).
- [26] P. Gaspard and D. Andrieux, *J. Chem. Phys.* **141**, 044908 (2014).
- [27] R. Rao and M. Esposito, *New J. Phys.* **20**, 023007 (2018).
- [28] P. Sartori and S. Pigolotti, *Phys. Rev. Lett.* **110**, 188101 (2013).
- [29] R. Rao and L. Peliti, *J. Stat. Mech.: Theor. Exp.* (2015) P06001.
- [30] A. Murugan, D. A. Huse, and S. Leibler, *Proc. Natl. Acad. Sci. U.S.A.* **109**, 12034 (2012).
- [31] M. Johansson, M. Lovmar, and M. Ehrenberg, *Curr. Opin. Microbiol.* **11**, 141 (2008), cell Regulation.

- [32] Y. Savir and T. Tlusty, *Cell* **153**, 471 (2013).
- [33] J. Zhang, K.-W. Jeong, M. Johansson, and M. Ehrenberg, *Proc. Natl. Acad. Sci. U.S.A.* **112**, 9602 (2015).
- [34] Y. Shimizu, T. Kanamori, and T. Ueda, *Methods* **36**, 299 (2005), engineering Translation.
- [35] S. Uemura, R. Iizuka, T. Ueno, Y. Shimizu, H. Taguchi, T. Ueda, J. D. Puglisi, and T. Funatsu, *Nucleic Acids Res.* **36**, e70 (2008).
- [36] H. R. Lee and K. A. Johnson, *J. Biol. Chem.* **281**, 36236 (2006).
- [37] K. Shimizu, K. Hashimoto, J. M. Kirchner, W. Nakai, H. Nishikawa, M. A. Resnick, and A. Sugino, *J. Biol. Chem.* **277**, 37422 (2002).
- [38] L. M. Dieckman, R. E. Johnson, S. Prakash, and M. T. Washington, *Biochem.* **49**, 7344 (2010).
- [39] K. Hashimoto, K. Shimizu, N. Nakashima, and A. Sugino, *Biochemistry* **42**, 14207 (2003).
- [40] M. Hashimoto, T. Nozoe, H. Nakaoka, R. Okura, S. Akiyoshi, K. Kaneko, E. Kussell, and Y. Wakamoto, *Proc. Natl. Acad. Sci. U.S.A.* **113**, 3251 (2016).
- [41] M. Johansson, J. Zhang, and M. Ehrenberg, *Proc. Natl. Acad. Sci. U.S.A.* **109**, 131 (2012).
- [42] H. B. Callen and T. A. Welton, *Phys. Rev.* **83**, 34 (1951).
- [43] R. Balescu, *Equilibrium and Non-Equilibrium Statistical Mechanics*, Wiley-Interscience (John Wiley & Sons, New York, 1975).